33rd Annual International Conference of the IEEE EMBS
Boston, Massachusetts USA, August 30 - September 3, 2011

The Response of Hepatocyte Cell Volume to Hyperthermia and its Role in Oedema

D.P. O'Neill, T. Peng, & S.J. Payne

Institute of Biomedical Engineering, Department of Engineering Science,
University of Oxford, Oxford, UK, OX1 3PJ
david.oneill@eng.ox.ac.uk

***Abstract*—A novel mathematical model for hepatocytes and surrounding volume is presented here; in addition to tracking ion transport and diffusion the new model allows for changing cell volume. Using temporally and spatially varying temperature as an input, this paper shows how differences between diffusion coefficients directly influence increases in cell volume. The multiscale nature of the model presents a possible link from established cellular equations to the observed clinical result of oedema present in thermal treatments of cancer.**

I. INTRODUCTION

The hepatocyte is the primary cell of liver tissue, accounting for 60% of cells and 80% of volume [1]. Its functions include metabolism, bile treatment and exchange of ions, which are essential for the body to maintain homeostasis. For these tasks to function correctly, steady-state behaviour of the hepatocyte that maintains the correct balance between intracellular and extracellular ion concentrations is particularly important.

Many equations that govern the behaviour of both passive and active transport of ions across the cell membrane involve a dependence upon temperature, often in the following form: $exp\left(\frac{ve}{kT}\right)$, where v is a potential, e is the elementary charge, k is Boltzmann's constant, and T is the temperature. Equations used to model ion transport are thus often nonlinear and produce complex relationships between cell temperature status.

Thermal treatments for liver cancer are becoming increasingly common as alternatives to liver resection; the aim being to raise tissue regions to a temperature sufficient to kill tumour cells. However, an inevitable effect of heat transfer is that there will be temperature rises in regions of tissue peripheral to the thermal target.

It has been observed [2] that tissue swelling occurs as a result of ablation treatments. Swelling is the influx of fluid, often a result of altered osmolarity — changed ion concentrations both inside and outside cells. Such an oedema is a likely indication of an abnormal, local adjustment of homeostatic conditions. Understanding the cell volume response to temperature could help in interpreting responses to ablation treatments on a tissue level.

In this paper, an existing cell model is adapted to simulate a single hepatocyte in an extracellular liver volume. Equations proposed by Endresen et al. [3] are adjusted to fit with reported hepatocyte conditions and the model is made multiscale by considering a permeable continuum of hepatocytes. The system is then subjected to spatially varying, dynamic temperature conditions in order to investigate tissue-level oedematic responses.

II. MODEL

Considering the cell as shown in Fig. 1, the system has seven variables: (V_e, V_i, Na_e, K_e, Na_i, K_i, and v), which are, respectively, extracellular volume, intracellular volume, extracellular sodium and potassium concentrations, intracellular sodium and potassium concentrations, and cell membrane potential. There also exist a constant number of large, inactive ions in the cell volume, the variable concentration, A_i, is eliminated subsequently.

A. Volume

Considering an arbitrary constant unit volume, V, the continuity of volume can be expressed as:

$$V_i/V + V_e/V = 1 = \phi_i + \phi_e, \tag{1}$$

where ϕ_i and ϕ_e are non-dimensional volume fractions.

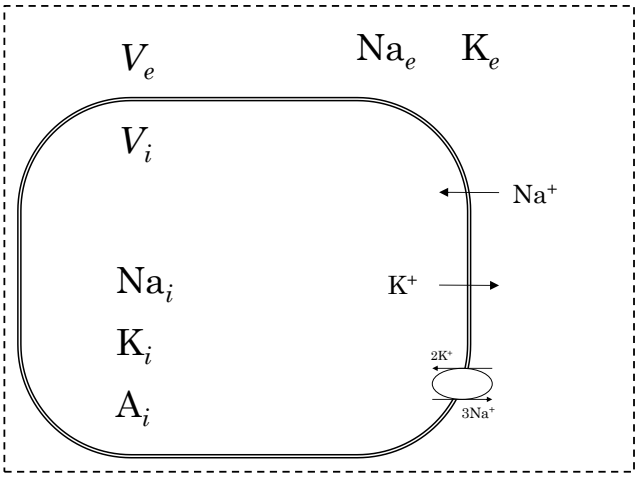

Fig. 1. Model schematic showing ion species, and transport mechanisms across the cell membrane

B. Ion Currents

In this simplified model, ions can be transported across the cell membrane by way of sodium channels, potassium channels and the sodium-potassium pump. By considering steady-state operation and using equations provided by Endresen et al. [3], the currents for the transport mechanisms are given as:

$$i_{\mathrm{K}} = k_{\mathrm{K}} \frac{1}{2} \left(1 + \tanh\left(\frac{2e\left(v - v_x\right)}{kT}\right)\right) \times \sinh\left(\frac{e\left(v - v_{\mathrm{K}}\right)}{2kT}\right), \tag{2}$$

$$i_{\mathrm{Na}} = k_{\mathrm{Na}} \frac{1}{4} \left(1 - \tanh\left(\frac{2e\left(v - v_h\right)}{kT}\right)\right) \times \left(1 + \tanh\left(\frac{2e\left(v - v_m\right)}{kT}\right)\right) \sinh\left(\frac{e\left(v - v_{\mathrm{Na}}\right)}{2kT}\right), \tag{3}$$

and

$$i_{\mathrm{NaK}} = k_{\mathrm{NaK}} \tanh\left(\frac{v + 2v_{\mathrm{K}} - 3v_{\mathrm{Na}} - v_{\mathrm{ATP}}}{\frac{2kT}{e}}\right), \tag{4}$$

where k_{K}, k_{Na}, and k_{NaK} are conductance parameters, v_x and v_m are half-activation potentials of the x and m gates, v_h is the half-inactivation potential of the h gates, and v_{ATP} is the potential corresponding to the Na-K pump action.

In steady-state there can be no accumulation of either ion inside the cell. The Na-K pump removes $3\mathrm{Na}^+$ from the cell whilst drawing in $2\mathrm{K}^+$ and thus the conservation of ions can be expressed as:

$$-3i_{\mathrm{NaK}} - i_{\mathrm{Na}} = 0, \tag{5}$$

and:

$$2i_{\mathrm{NaK}} - i_{\mathrm{K}} = 0. \tag{6}$$

C. Osmotic Pressure

The osmotic pressure across the cell wall must be zero if mechanical forces within the cell wall are neglected, thus at equilibrium:

$$\frac{\partial}{\partial t}\left(\mathrm{Na}_e + \mathrm{K}_e\right) = \frac{\partial}{\partial t}\left(\mathrm{Na}_i + \mathrm{K}_i + \mathrm{A}_i\right). \tag{7}$$

Whilst the concentration, A_i, can vary, the total number of ions present cannot, and so the following substitution can be utilised:

$$\mathrm{A}_i = \mathrm{A}_i^0 \phi_i^0 / \phi_i, \tag{8}$$

where the superscript 0 denotes baseline (normothermic) values.

D. Extracellular Electro-neutrality

The net charge of the extracellular volume in the model is kept constant, which yields:

$$\mathrm{Na}_e + \mathrm{K}_e = \mathrm{Na}_e^0 + \mathrm{K}_e^0. \tag{9}$$

E. Extracellular Diffusion

The unit volume of Fig. 1 is part of a continuum of permeable tissue, through which ions can passively travel. In the absence of significant advection, diffusion dominates ion motion in the extracellular volume. Conservation of ions yields the expression:

$$\frac{\partial}{\partial t}\left(\phi_e \mathrm{Na}_e\right) = \nabla D_{\mathrm{Na}} \nabla \mathrm{Na}_e + S_{\mathrm{Na}}, \tag{10}$$

where D_{Na} is a spatially variable diffusion coefficient and S_{Na} is a source term which accounts for the efflux of ions into the extracellular volume from inside the cell. This source term is thus:

$$S_{\mathrm{Na}} = -\frac{\partial}{\partial t}\left(\phi_i \mathrm{Na}_i\right). \tag{11}$$

The reported coefficients of diffusion correspond to the volume fractions at baseline values and so with variable volume fraction, the variable coefficients can be substituted by:

$$D_{\mathrm{Na}} = \frac{\phi_e}{\phi_e^0} D_{\mathrm{Na}}^0, \tag{12}$$

Using the non-dimensionalising substitutions $t' = t/\tau$ and $r' = r/R$, 10 can be re-expressed as:

$$\frac{\partial}{\partial t'}\left(\phi_e \mathrm{Na}_e + \phi_i \mathrm{Na}_i\right) = \nabla \frac{\phi_e}{\phi_e^0} D_{\mathrm{Na}}^0 \frac{R^2}{\tau} \nabla \mathrm{Na}_e, \tag{13}$$

from which, a non-dimensional coefficient of diffusion can be taken as:

$$D'_{\mathrm{Na}} = \frac{R^2}{\tau} D_{\mathrm{Na}}^0 \tag{14}$$

A corresponding set of expression for potassium ions make up the seventh, and final, equation of the model.

III. Model Analysis

A. Model Computation

With 7 variables and 7 equations, the system was solved by differentiating 1, 5, 6, 7 and 9 with respect to time (for reasons of space these differentials are not included here) and then arranged into the form:

$$\mathbf{M}\dot{\mathbf{u}} = \mathbf{F}_{diff}\left(\mathbf{u}\right) + \mathbf{F}_{temp}\left(\mathbf{u}\right), \tag{15}$$

where $\mathbf{M}$ is a mass matrix for the temporal derivative vector of seven variables, $\mathbf{u}$, whilst $\mathbf{F}_{diff}\left(\mathbf{u}\right)$ is a forcing function from the extracellular diffusion. $\mathbf{F}_{temp}\left(\mathbf{u}\right)$ is a forcing function that depends upon u and the temporal derivatives of temperature.

The model considers a 1-D spherical polar coordinate space, which means that 10 becomes:

$$\nabla \frac{\phi_e D_{\mathrm{Na}}^0}{\phi_e^0} \nabla \mathrm{Na}_e = \frac{\partial}{\partial r} \frac{\phi_e D_{\mathrm{Na}}^0}{\phi_e^0} \frac{\partial}{\partial r} \mathrm{Na}_e + \frac{2}{r} \frac{\phi_e D_{\mathrm{Na}}^0}{\phi_e^0} \frac{\partial}{\partial r} \mathrm{Na}_e, \tag{16}$$

and a similar expression exists for potassium. Computationally, the linearity of the diffusion equation allows for the spatial derivative terms to be discretised and the system solved using the 'method of lines' [4]. Equation 15 can then be solved in MATLAB with a stiff ODE solver to manage the non-linearities of the system.

For simulations, the $\mathbf{F}_{temp}(\mathbf{u})$ source term was used as the input and a function was selected to be continuous in space and time ($\partial T/\partial t$ must be computable).

B. Temperature Function

For the simulations, the system was subjected to a temperature distribution that is continuous in space and time. To simulate a spatial variation that might appear clinically, the temperature function was spatially dependent by:

$$\mathbf{F}_{temp,r}(r') \propto \frac{1}{2}\left(1-\tanh\frac{r'-r_c}{r_{stretch}}\right), \tag{17}$$

where r_c sets an offset of the centrepoint for the 'turn off' of the spatial distribution, and $r_{stretch}$ scales the stretch of the spatial distribution. Similarly, modified hyperbolic tangent functions were used to 'turn on' and subsequently 'turn off' the heating function in time.

$$\mathbf{F}_{temp,t}(t') \propto \frac{1}{2}\left(1+\tanh\frac{t'-t_{c,1}}{t_{stretch,1}}\right)\left(1-\tanh\frac{t'-t_{c,2}}{t_{stretch,2}}\right), \tag{18}$$

where $t_{c,1}$ and $t_{c,2}$ set the offsets of the centrepoints, and $t_{stretch,1}$ and $t_{stretch,2}$ scale the stretches. The temperature function is therefore the product of the spatial and temporal components and also of a peak magnitude of heating, T_{max}:

$$\mathbf{F}_{temp}(t',r') = T^0 + T_{max}\mathbf{F}_{temp,r}(r')\,\mathbf{F}_{temp,t}(t'). \tag{19}$$

C. Parameter Values

In the model, the volume of the cell accounts for 80% of the volume, i.e. $\phi_i = 0.8$ and $\phi_e = 0.2$. Parameters values given by Endresen et al. for v_x, v_m, v_h, and v_{ATP} were unaltered. The liver has different ion concentrations to those reported by Endresen et al. for atrial cells, and consequently Nernst potentials for liver also differ from those for atrial cells. In order to satisfy 5 and 6 two of the adjustable conductance parameters, k_{Na} and k_{K}, were modified. Baseline coefficients of diffusion were taken from McLennan's [5] findings, in each case, multiple values were reported and the mean was used. Values of intra- and extracellular ion concentrations were given by Melkikh and Sutormina [6]; however, to generate valid Nernst potentials, it was necessary to adjust the concentrations. Values for Na_e, K_e, and Na_i were not altered, whilst K_i was lowered from 166 mM to 128 mM. Finally, a starting point value for A_i was taken from Matthews [7], and was also reduced — from 108 mM to 91.8 mM.

Values used are listed in full in Table 1.

TABLE I
VALUES FOR PARAMETERS AND CONSTANTS REQUIRED FOR SIMULATIONS

Variable/Constant	Value	Unit	Source
k	1.38×10^{-20}	mJ K^{-1}	Constant
e	1.60×10^{-19}	C	Constant
R	8310	J kmol^{-1} K^{-1}	Constant
Na_e^0	143	mM	[6]
K_e^0	4.0	mM	[6]
Na_i^0	29.0	mM	[6] (adjusted)
K_i^0	128	mM	Recalculated
A_i^0	91.8	mM	[7] (adjusted)
k_{Na}	27100	pA	Recalculated
k_{K}	1060	pA	Recalculated
k_{NaK}	11.5	pA	[3]
v_x	-25.1	mV	[3]
v_h	-91.0	mV	[3]
v_m	-41.4	mV	[3]
v_{ATP}	-450	mV	[3]
ϕ_i^0	0.8	$\mathrm{cm}^3/\mathrm{cm}^3$	[5]
D_{Na}^0	10.5×10^{-4}	cm^2 min^{-1}	[5] (averaged)
D_{K}^0	3.7×10^{-4}	cm^2 min^{-1}	[5] (averaged)
τ	1.0	min	n.a.
R	1.0	cm	n.a.

IV. Model Simulation Results

Using a maximum temperature rise (T_{max}) of +70 K and values for r_c, $r_{stretch}$, $t_{c,1}$, $t_{c,2}$, $t_{stretch,1}$, and $t_{stretch,1}$ of 1, 1, 10, 70, 5, and 5 respectively, the resultant temperature profile imposed on the system is shown in Fig. 2, whilst Fig. 3 shows a plot of $\frac{\partial T}{\partial t}$. The simulation yields results as shown in Fig. 4. An increase in cell volume is clearly evident close to the origin, where there is a 10% reduction in extracellular volume.

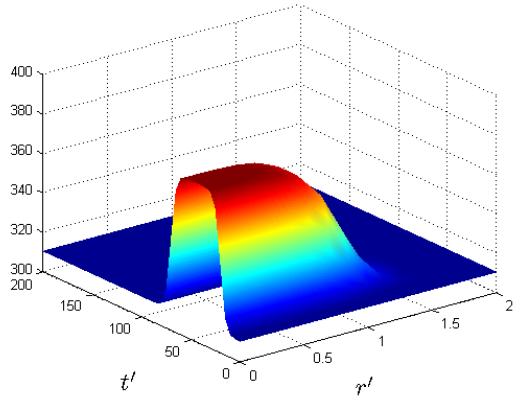

Fig. 2. Temperature profile imposed on system simulating likely conditions of a thermal treatment scenario.

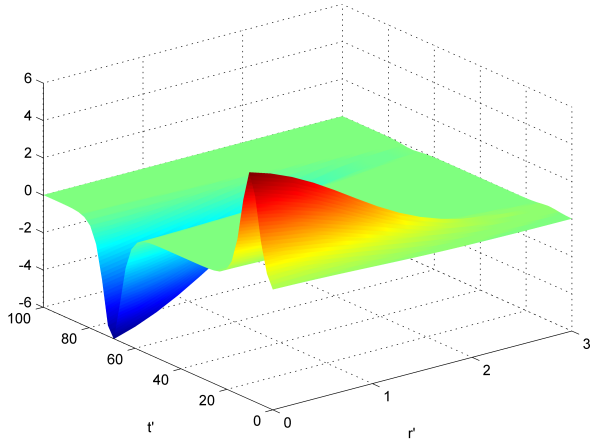

Fig. 3. Temporal derivative ($\frac{\partial T}{\partial t}$) of temperature profile imposed on system, and main driving function of the model.

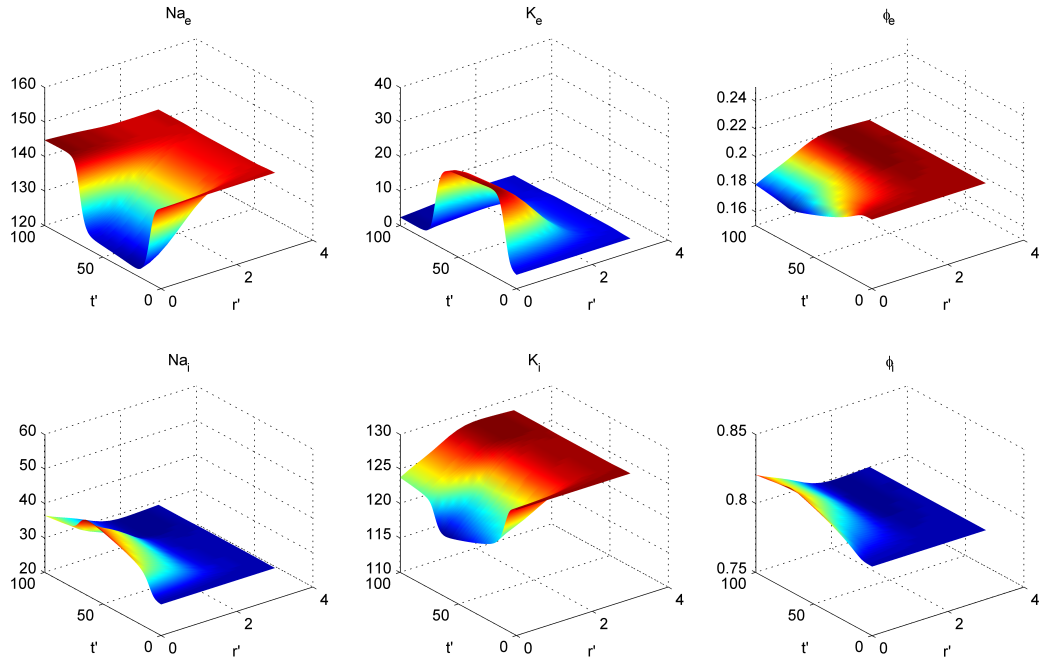

Fig. 4. Simulation results for parameters given in text. Top panels (left to right) show Na_e, K_e, and ϕ_e. Bottom panels (left to right) show Na_i, K_i, and ϕ_i.

V. Discussion and Future Work

With the above simulation it has been possible to show how cell volume may increase as a result of a rise of temperature. The model demonstration uses a single temperature function. Variations in this function will prove insightful as to determine the most important features of such functions, in particular whether the rate of temperature rise is significant in determining the response of cell volume.

It is important to note here, that the imposed temperature distribution contains a maximum temperature of 100 °C. Such high temperatures for long durations will result in cell death; where this model may become of significant use is in the investigation of areas peripheral to an ablation lesion. It is often in the annular region of tissue surrounding the treatment target volume that oedemata are most important. Interpreting treatment effects in such areas is one of a clinician's highest priorities as there is a significant knowledge gap between observing oedemata and predicting the treatment outcome of associated temperature rises.

There exist a number of areas for model refinement. Perhaps the most significant is that the model as shown in Fig. 1 incorporates only 3 species of ion. Real cells are far less simplistic and require more detailed models. Notably, chloride ions are frequently considered as significant; future refinement of this model should include investigations into the expanding the set of equations to incorporate additional species.

VI. Conclusions

The model presented here demonstrates a possible multiscale explanation for oedemata that occur during thermotherapy. Established equations for ion transport across the cell membrane were adapted from atrial cells to hepatocytes, and new variables were included to permit swelling and shrinkage of the cell. The model was made to be multiscale by incorporating the tissue-level process of extracellular diffusion of ions. By subjecting this novel model to a dynamic temperature distribution, representative of that imposed during thermal treatments, it was found that significant cell swelling occurs. These results suggest that standard cellular operation at abnormal, hyperthermic, conditions might play a part in the clinically observed side-effect of oedema.

References

[1] H. Gray, *Gray's Anatomy: The Anatomical Basis of Medicine & Surgery*, Churchill Livingston; 38th edition, 1995

[2] G. Antoch et al. , Assessment of Liver Tissue After Radiofrequency Ablation: Findings with Different Imaging Procedures, *J. Nucl. Med.* vol. 46, 2005, pp 520-525.

[3] L.P. Endresen, K. Hall, J.S. Høye, and J. Myrheim, A Theory for the Membrane Potential of Living Cells, *Eur. Biophys. J.*, vol. 29, 2000, pp 90-103.

[4] W.E. Schiesser and G.W. Griffiths, *A Compendium of Partial Differential Equation Models*, Cambridge University Press, New York, NY; 2009.

[5] H. McLennan, The Diffusion of Potassium, Sodium, Sucrose and Inulin in the Extracellular Spaces of Mammalian Tissues, *Biochemica et Biophysica Acta*, vol. 24, 1957.

[6] A.V. Melkikh and M.I. Sutormina, A Model of Active Transport of Ions in Hepatocytes, *Biophysics*, vol. 55, 2010, pp 67-70.

[7] G.G. Matthews, *Cellular Physiology of Nerve and Muscle*, Blackwell Publishing, Oxford, UK; 2009